COMPARISON OF CHIRP SCHEMES FOR SHORT-PULSE X-RAY BEAMS IN LIGHT SOURCES*

L. Emery†, M. Borland, A. Zholents, ANL, Argonne, IL 60439, USA

Abstract

The Advanced Photon Source (APS) is planning [1] to produce a short-pulse x-ray beam by way of rf deflecting cavities that locally impose a y'-t correlation on the stored beam at an insertion device. SPring-8 recently proposed [2] a variation on this scheme whereby the deflecting cavities impose a local y-t correlation on the stored beam. In one case the chirp is in the angle coordinate and in the other case the position coordinate. They both use slits to pass through a "short" portion of the photon beam. The practical limitations for the two schemes are discussed and compared, such as photon source size and angular divergence, storage ring apertures, and slit transmission.

INTRODUCTION

In the SPX scheme[3] we propose for APS, the insertion device (ID) is located at a vertical phase advance of $n180°$ from the cavities, where $n \geq 0$ is an integer. As a result, the ultimate x-ray pulse length that is achievable in this scheme is limited by the vertical electron beam divergence and the intrinsic opening angle of the radiation, as well as the deflecting voltage slope [4]. We'll call this the momentum-based scheme.

A modified configuration [2], which we'll call the position-based scheme, is possible that makes use of a spatial electron beam chirp. This can be implemented by having a four-cavity bump in a very long straight section, or by placing an undulator at a phase advance of $(2n+1)90°$ from the cavities (where $n \geq 0$). In this case, the relevant comparison is of the size of the chirp to the vertical electron beam size and the intrinsic size of the radiation source. In ID straight sections, the former tends to be small because of the small vertical beta function needed to accommodate the vacuum chamber. The latter is given by (see below) $\frac{1}{4\pi}\sqrt{\pi\lambda_r L_u}$, where λ_r is the wavelength emitted and L_u is the length of the insertion device. For 1 Å radiation, this is about 10% of the typical vertical beamsize at an ID in the APS. Together, these seem to promise shorter x-ray pulses with less chirp, albeit with lower intensity (since one is still performing slicing).

We'll look at the option of putting the cavities in a long straight section at the APS, even though our straight sections isn't as long as SPring-8's longest. Alternatively, one could modify the APS optics to achieve 90-degree vertical phase advance between three successive straight sections. However, this requires large vertical beta functions in the middle straight section and is not workable.

* Work supported by the U.S. Department of Energy,Office of Science, Office of Basic Energy Sciences, under Contract No. DE-AC02-06CH11357.

† lemery@aps.anl.gov

COMPARISON

Figure 1 shows the different cavity and drift space layouts for applying an momentum chirp or a position chirp. Arrows show whether there is vertical momentum at the end slices of the bunch. The position chirp scheme requires

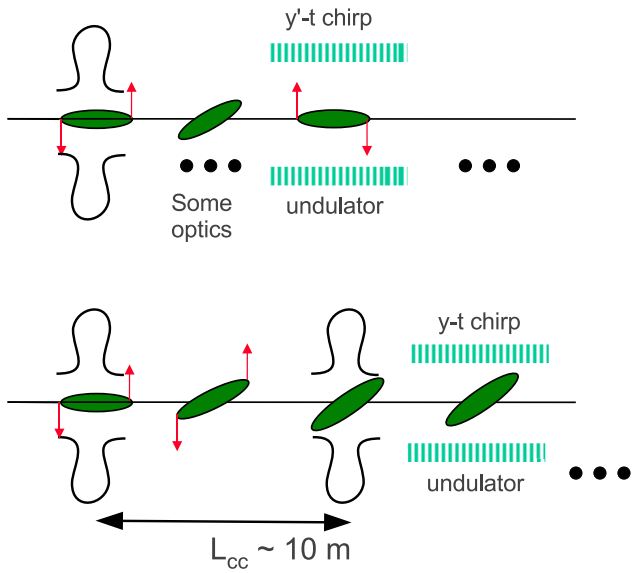

Figure 1: Layouts for applying a momentum chirp (top) and position chirp (bottom).

a long straight section that can accommodate four cavities plus the insertion device. Two cavities (or groups of cavities) are placed on either side of the insertion device. The first set of cavities create an angular chirp, which after a long drift is converted to a spatial chirp. At this point, the second set of cavities zero-out the angular chirp, thus locking in the spatial chirp. Next, the beam goes through the insertion device, following which two more sets of cavities undo the chirp (not shown).

Before making accurate calculations of x-ray pulse length, one can examine the expressions for the case of infinitesimally-small slits (zero-slit-size limit):

$$\sigma_t = \frac{E}{2\pi h f_{\rm rf} V}\sigma_{y'}^{\rm eff} \qquad \text{for } y'-t \text{ chirp} \qquad (1)$$

$$\sigma_t = \frac{E}{2\pi h f_{\rm rf} V}\frac{\sigma_y^{\rm eff}}{L_{cc}} \qquad \text{for } y-t \text{ chirp} \qquad (2)$$

where E is the energy of the beam, $hf_{\rm rf}$ is the frequency of the deflecting cavities, V is the integrated kick voltage of

the first cavity in each case, $\sigma_{y'}^{\text{eff}}$ and $\sigma_{y'}^{\text{eff}}$ are the effective beam size and angular spread of the photons emitted when $V = 0$, and L_{cc} is the distance between each pair of cavities in the position chirp case. Thus we have to compare the details of $\sigma_{y'}^{\text{eff}}$ and $\sigma_{y}^{\text{eff}}/L_{cc}$.

We also need estimates of the effective single-electron size and divergence for undulator radiation. The full-width opening angle of the radiation within the spectral bandwidth $\Delta\lambda/\lambda = 1/N$ is [5] $\theta_{\text{cen}} = \sqrt{2\lambda_r/L_u}$, implying

$$\sigma_\theta = \sqrt{\frac{\lambda_r}{\pi L_u}}. \tag{3}$$

Using $\varepsilon_r = \sigma_r\sigma_\theta = \lambda/(4\pi)$ gives

$$\sigma_r = \frac{1}{4\pi}\sqrt{\pi L_u \lambda_r} \tag{4}$$

and $\beta_r = \sigma_r/\sigma_\theta = L_u/4$.

For the momentum chirp

$$\sigma_{y'}^{\text{eff}} = \sqrt{\frac{\varepsilon_y}{\beta_y}}\sqrt{1 + \frac{\varepsilon_r}{\varepsilon_y}\frac{\beta_y}{\beta_r}}, \tag{5}$$

where ε_y is the vertical emittance, β_y is the vertical beta function. The first term on the right-hand side is fixed by emittance of the accelerator and the beta function, which is determined by the aperture. Hence, it is fixed when the radiation or undulator change. Assuming the undulator fills half the straight section and optimum beta functions for the aperture, we have $\beta_y = (2L_u)/2 = 4\beta_r$. Hence, we can simplify Equation 5:

$$\sigma_{y'}^{\text{eff}} \approx \sqrt{\frac{\varepsilon_y}{\beta_y}}\sqrt{1 + \frac{4\varepsilon_r}{\varepsilon_y}}. \tag{6}$$

Hence, the best use of this technique is when

$$\varepsilon_y \gtrsim 4\varepsilon_r \rightarrow \lambda_r \lesssim \pi\epsilon_y. \tag{7}$$

For APS, with $\varepsilon_y = 35$ pm, this implies $\lambda_r \lesssim 1$ Å.

For the position chirp

$$\frac{\sigma_y^{\text{eff}}}{L_{cc}} = \frac{\sqrt{\varepsilon_y\beta_y}}{L_{cc}}\sqrt{1 + \frac{\varepsilon_r}{\varepsilon_y}\frac{\beta_r}{\beta_y}} \tag{8}$$

where again the term $\sqrt{\varepsilon_y\beta_y}$ is fixed for purposes of comparison. Note that typically $\beta_y \approx L_{cc}$, since $2L_{cc}$ is roughly the straight section length, while $L_u \lesssim FL_{cc}$, with $F < 1$. Hence, the best use of this technique is when

$$\lambda_r \lesssim \frac{4\pi\varepsilon_y}{F}. \tag{9}$$

We expect this method to give superior results when λ_r is large. For APS, it would extend the range of good performance to $\lambda_r \lesssim 10$ Å or better.

Note that magnet optics in arcs or straight section could somewhat enhance both schemes by way of factors not included in Equations 1 and 2. Also in position chirping, one could use quadrupole optics in a long straight section to enhance the effect, and forgo building two of the four cavities. This had not been investigated though it would require 180° in phase advance. However, this entails dealing with chromaticity and other issues[4], the avoidance of which is one of the benefits of the position-based scheme.

Not included is a study of apertures which would limit the chirp in both cases, perhaps more so in the position chirp case since the large projected vertical beam size occurs entirely in the ID chamber.

These formulae give the limiting pulse length. Of course we must apply realistic conditions, which comes next.

CONFIGURATION FOR APS

Position chirp would have the advantage of eliminating some of the beam dynamics issues associated with the original scheme[4]. If we implemented this scheme in APS with a 7.7-m-long straight section, we might be able to fit six cavities on either side of a 2.4-m-long ID. (Overall, about 2.65 m is available for cavities on each side of the ID.) Hence, we grouped the cavities into four sets of three. Each cavity was assumed to have length $\lambda/2 \approx 0.053$ m and to be padded by a drift region of length $3\lambda/2$ on each side. This left about 1 m between the cavity sets on each side of the ID.

SIMULATION

The simulations were performed with `elegant` [6]. Because the chirp is confined to a single straight section, we simulated only that straight section. The lattice consisted of `RFDF` elements (for the cavities) and drift spaces. In all cases, a total of 16 single-cell deflecting cavities are used with a deflecting voltage of 0.5 MV each. We used bunch durations of 33 and 50 ps, corresponding to the present bunch length in 24 bunch mode and the predicted bunch length [7] at 200 mA in 24 bunch mode with the impedance of the cavities included.

After tracking, we used a simple script and SDDS tools [8] to add the radiation divergence or beamsize, depending on the scheme, using the Gaussian approximation, then perform a slit scan. For the position-based scheme, this is somewhat idealized because we are ignoring the beam divergence. However, with point-to-point imaging optics to the slit, this should be a good assumption.

Figure 2 shows the results for momentum-based configuration using several different radiation wavelengths. The quantity "Dt70" is the time width that holds the central 70% of the photons. It is virtually equal to the FWHM for a Gaussian distribution, but more statistically robust in a simulation. As expected, performance degrades when the wavelength is longer than a few Å. However, for hard x-rays, we approach 1 ps FWHM with about 1% transmission.

Figure 3 shows the results for the position-based scheme at several radiation wavelengths. For 1 Å, the minimum

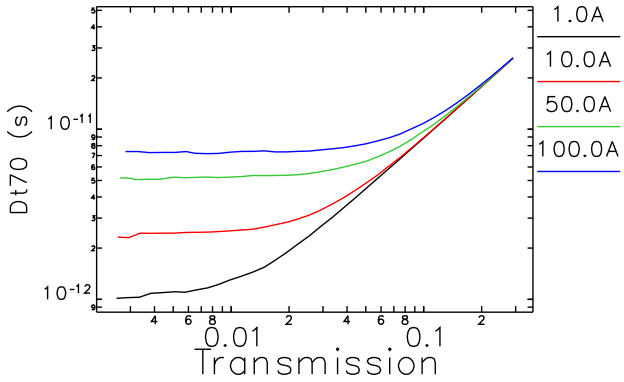

Figure 2: Slit scan for 50 ps electron bunch duration and three radiation wavelengths, assuming the momentum-based scheme.

FWHM pulse duration is about 3 ps with 1 to 2% transmission, which is not as good as the momentum-based scheme. The momentum-based scheme continues to perform best for radiation wavelengths up to about 50 Å.

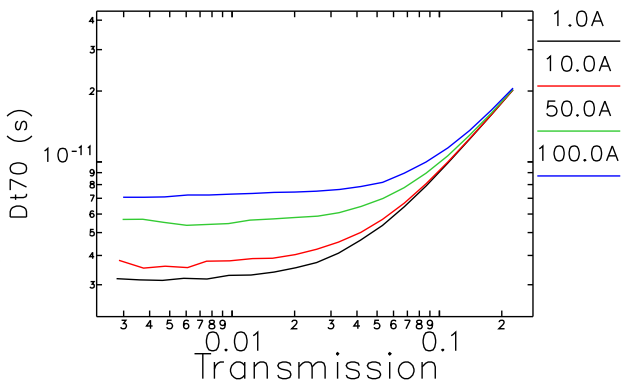

Figure 3: Slit scan for 50 ps electron bunch duration and three radiation wavelengths, assuming the position-based scheme in a 7.7-m straight section. Results for 33 ps bunch are virtually the same.

We further analyzed the performance of the position-based scheme for a super-long straight section of 11.9 (per Case 4 in [9]). While this would be quite expensive, it is useful as an extreme case. The results are shown in Figure 4. These are essentially as good (within 50%) as the short-wavelength results from the momentum-based scheme, shown in Figure 2. The long-wavelength values are much improved, as expected.

CONCLUSION

We've compared the position-based scheme to the momentum-based scheme for application to short x-ray pulse production at the APS. For the straight section length that is available, we find that the momentum-based scheme produces shorter pulses for the same transmission and number of cavities, assuming 50 Å or shorter wavelength.

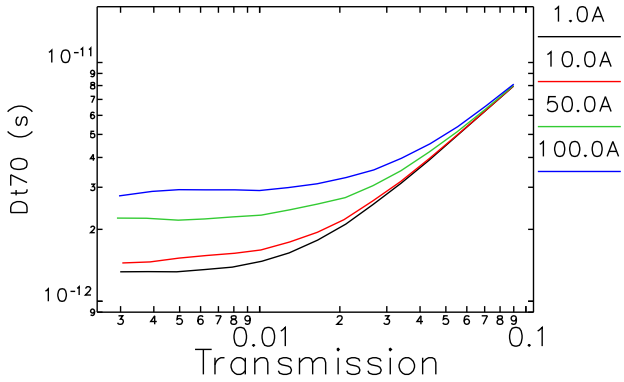

Figure 4: Slit scan for 50 ps electron bunch duration and three radiation wavelengths, assuming the position-based scheme in an 11.9-m straight section. Results for 33 ps bunch are virtually the same.

However, for softer x-rays, the position-based scheme has an advantage. However, if we install a super-long straight section, which involves shorter dipole magnets, the position-based scheme performs essentially the same as the momentum-based scheme for hard x-rays and much better for soft x-rays. However, for approximately the same cost, the original scheme allows us to provide chirped pulses to three ID and two magnet beamlines, compared to only one ID beamline for the position-based scheme. Note that the soft x-ray users can obtain shorter pulses at the bending magnet beamlines than at the ID beamlines.

REFERENCES

[1] A. Nassiri, these proceedings.

[2] T. Fujita et al., Proc. of 2010 IPAC, 39 (2010).

[3] A. Zholents et al., NIM A, **425**, 385, (1999).

[4] M. Borland, PRST-AB, **8**(7), 074001, (2005).

[5] D. Attwood. Soft X-rays and Extreme Ultraviolet Radiation. Cambridge University Press, 2000.

[6] M. Borland. Technical Report LS-287, Advanced Photon Source, (2000).

[7] Y. Chae. Private communication, (2010).

[8] R. Soliday et al., Proc. 2003 PAC, 3473 (2003).

[9] Study of Long Straight Section for IXS-CAT. `http://www.aps4.anl.gov/operations/ops_www/APSOnly/LongStraightSection/%LongStraightSection.html`.